This work used soursop as a green corrosion inhibitor to protect API 5L Grade A from detrimental corrodent under produced water. Despite the effectiveness of inorganic inhibitors, recent evidence on their toxicity test suggests that implementing organic inhibitors is substantial to replace synthetic corrosion inhibitors. However, soursop utilization as a green corrosion inhibitor is poorly understood due to the lack of a comprehensive extraction mode and inhibitive mechanism. Several tests were conducted, including weight loss, potentiodynamic polarization, and electrochemical impedance spectroscopy (EIS), to unveil the nature of corrosion inhibition. Fourier Transform Infra-Red Spectroscopy revealed the dominant functional groups to bind with the substrate. The potentiodynamic polarization results show that the inhibitor is a mixed-type inhibitor that influences the anodic and cathodic reactions. The weight loss test showcases the highest inhibition efficiency of 52.62 % upon adding 2 ml inhibitors upon eight observation days. The polarization and EIS results provide that the inhibitor reduces the corrosion rate with higher inhibition of 88.52 %. The mentioned result is associated with the attachment of non-polar and polar Annona muricata Linn functional groups. The primary functional group involves C=O, C–C and –O.H., which actively bonded to the metal's surface. The aromatic group at a wavenumber of 1,050 and 1,090 cm^{-1} shows ether's presence and behaves as an adsorption center. In this work, combining three solvents, hexane, acetone, and ethanol, elicits the complete extraction of the predominant compound from soursop.

Keywords: green corrosion inhibitors, organic corrosion inhibitors, Annona muricata Linn, soursop adsorption inhibition

UDC 541
DOI: 10.15587/1729-4061.2023.278911

DEVELOPMENT OF ANNONA MURICATA LINN AS GREEN CORROSION INHIBITOR UNDER PRODUCED WATER: INHIBITION PERFORMANCE AND ADSORPTION MODEL

Ayende
Doctor of Engineering
Department of Mechanical Refinery Engineering
PEM Akamigas
Jalan Gajah Mada, 38, Cepu, Blora, Jawa Tengah, Indonesia, 58315
Rini Riastuti
Doctor of Engineering, Senior Lecturer*
Johny Wahyuadi Soedarsono
Corresponding author
Doctor of Engineering, Professor*
E-mail: jwsono@metal.ui.ac.id
Agus Paul Setiawan Kaban
Master of Engineering, Graduate Student*
Mohammad Ikbal Hikmawan
Master of Engineering
PT Pertamina Hulu Energy
Jl. TB Simatupang No. Kav. 99, RT.1/RW.1, Kebagusan, Ps. Minggu, Kota Jakarta Selatan, Daerah Khusus Ibukota Jakarta, Indonesia, 12520
Rizal Tresna Rahmdani
Bachelor of Science, Bachelor of Engineering, Master of Engineering, Senior Engineer*
*Prof Johny Wahyuadi Laboratory
Department of Metallurgical and Materials Engineering
Universitas Indonesia
Kampus Baru UI Depok, Jawa Barat, Indonesia, 16424

Received date 21.02.2023
Accepted date 27.04.2023
Published date 30.06.2023

How to Cite: *Ayende, Riastuti, R., Soedarsono, J. W., Kaban, A. P. S., Hikmawan, M. I., Rahmdani, R. T. (2023). Development of annona muricata linn as green corrosion inhibitor under produced water: inhibition performance and adsorption model. Eastern-European Journal of Enterprise Technologies, 3 (6 (123)), 56–65. doi: https://doi.org/10.15587/1729-4061.2023.278911*

1. Introduction

Corrosion remains a considerable challenge of the century and possesses business and environmental effects without significant intervention. Carbon steel remains the primary selected material widely used as a structural material due to its ductility and mechanical properties [1], especially in pipelines in offshore surface facilities. In the marine system, the likelihood of the material experiencing corrosion remains a significant issue, including exposure of the material to chloride ions and toxic CO_2 gas. Numerous field strategies have been implemented, such as inspection and corrosion monitoring, to slower the propagating effect of corrosion and deterioration of metals [2]. In practical activity, the injection of corrosion inhibitors influences the chemistry of transported fluid owing to their intervention in controlling the possible contact between the bare metals and corrodents. With this in mind, it is critical to ensure the protection of metals at an acceptable level using chemicals to lower the risk of metals exposure.

One of the primary issues in mitigating corrosion metal is the influence of by-products generated in the oil and gas process [3]. The report of [4] claims the produced water is provided when the underground water reaches the surface

facility during oil and gas exploration. It is also noteworthy to remember that the complexity of chemicals includes the organic and inorganic components. Further studies show that the ratio between water and oil is low at the beginning of oil and gas exploration despite a gradual rise as the well age grows [5]. A recent report showcases that the upstream process provides the optimum wastewater in both onshore and offshore well production. It denotes the condition of trapped water within oil and gas from geologic reservoirs for nearly a long time of observation [6].

The scarcity of corrosion prevention ultimately helps remove the pipeline from corrosion due to produced water. In comparison, it is critical to note that the possibility of corrosion is high when water and oxygen connect to metals. Another publication displays that the quantitative amount of water reaches 75–80 %, with the oil-to-water ratio within the range of 3:1 [7]. Hence, a simple strategy can be performed by disconnecting the line and treating the water to ensure the timed delivery of hydrocarbon to meet the energy demand. In these circumstances, green corrosion inhibitor injection privilege is critical to protect metals at an affordable business value.

In the previous research, the green corrosion inhibitor is an ideal chemical with a remarkable inhibitory effect while keeping the aquatic toxicity level low [8–10]. Several pieces of evidence elicit that a small dosage of inhibitors can broadly impact the corrosion process by controlling the corrosion process at the interface between metals and corrodents. Commonly, the extraction process becomes a challenge to gain nature's primary compounds. A few resources of inhibitors are plant extracts [11], ionic liquids [12], and medicines [13]. Amongst the resources, plant extract remains a primary substance aligned with the campaign of the green concept of corrosion inhibitor. Therefore, research devoted to developing soursop as a green corrosion inhibitor is relevant to unveil the excellent potential for corrosion prevention.

2. Literature review and problem statement

The paper [14] shows that energy demand has risen over more than ten years, including the mitigation of their facility. Shown that it is correlated to the prevention scheme of pipelines, the mitigation would bring extra benefits to the company. The reason for this may be linked to the preliminary assessment related to material integrity. It is critical to involve the injection of inhibitors. The recent development of inhibitors shows consideration for using green corrosion inhibitors to protect carbon steel. It is shown that the ultimate compounds, such as polyphenol from *Annona muricata Linn,* effectively inhibit corrosion due to the antioxidant activity [15]. However, the research may be an inherent fundamental impossibility without comparing the laboratory results with the actual coupon measurement to assess the effectiveness of inhibition. The reason for this can be their contaminants related to phytochemical compounds.

The research to unveil the potential of natural plants has been great attention to numerous studies. Table 1 summarizes the details of existing research in developing green corrosion inhibitors. Numerous studies have been given to unveil and harness the preceding discussion of natural plant-associated corrosion-related metal protection. The paper [16] argues that the adsorption characteristics of the inhibitor can be modeled using the thermodynamics-kinetic model. They use ethanol to extract the inhibitor from the bark roots of *Nauclea latifolia* to protect mild steel from the H_2SO_4 solution. Another concern is the achievement work [17] to recognize that roots and seeds extract of *Azadirachta indica* was utilized to characterize the corrosion protection under the same solution. Weight loss and gasometric techniques are sufficient to support the Freundlich adsorption isotherm result to conserve corrosion damage. The paper [18] arrests the degradation of metal protection by acquiring the extract of *Emblica officinalis* leaves. The study simulates that corrosion protection is prone to achieve its protection by evaluating corrosion rate using weight loss, potentiodynamic polarization and impedance studies.

Similarly, the research [19] shows *Combretum bracteosum* leaves the gravimetric method is suitable to protect mild steel from a low pH solution of H_2SO_4. According to their results, the inhibitor was a mixed-type class to achieve 97.5 % efficiency and abides by the Langmuir, Temkin, and Freundlich adsorption isotherm. The recent test [20] proves that the latex and fruit of *Calotropis procera* and *Calotropis gigantean* are moderately capable of depressing the corrosion rate of mild steel at 80 % efficiency. A recent study [21] shows *Citrus Aurantifolia* (CAL) leaves significantly impact mild steel under HCl 1M. They claim that the extract is classified as a mixed-type inhibitor. Moreover, the publication claims that ethanol is a suitable solvent to extract primary components of natural resources with the Diphenyl-1-picrylhydrazyl (DPPH) scavenging of 141.127 μg/ml. In the other study, the paper [22] confirms the presence of flavonoids, tannins, phytosterol, and alkaloids, which are essential to enhance the antioxidant activity of the soursop extract. The research claims that the capacity of the leaves and seeds of the plants is nearly 86 % and 39 %.

In this work, the adsorption process provides the principal possibility of using soursop extract as a green corrosion inhibitor. The green corrosion inhibitor usually comprises multiple high electronegative atoms such as oxygen, nitrogen, phosphorous, and sulfur [23]. In the same study, arene exhibits the resonance effect, enabling the donating electrons possible. The publication [24] states that using Secang heartwood effectively depletes the API 5L grade B corrosion rate under a 3.5 % NaCl environment with moderate inhibition of 53.18 %. The research [25] utilizes ascorbic acids despite being partially dissociated to give proton, which may contribute to corrosion. The research results show the sweet potato extract is ideal for reducing corrosion under the $FeCl_3$ environment.

An option to overcome the relevant difficulties to harness the potential of soursop as a green corrosion inhibitor is the extraction process and how they are compatible with reducing corrosion under produced water. It is the approach used in [26]; however, the research towards enhancing the protection of carbon steel API 5L Grade B remains in siloes. All this allows us to argue that a study devoted to unveiling the interaction between functional groups of soursop and the substrate is appropriate.

3. The aim and objectives of the study

The study aims to unravel the potential of soursop as a practical green corrosion inhibitor based on laboratory results and can be injected into the production well of oil and gas facilities.

To achieve this aim, the following objectives are accomplished:

– to investigate how the primary vibration of the soursop corrosion inhibitor correlates to their dominant functional groups;

– to study the inhibition performance of the soursop inhibitor related to how the component reduces the corrosion rate;

– to evaluate the adsorption isotherm of inhibition associated with their thermodynamic nature.

4. Materials and methods

4. 1. Object and hypothesis of the study

The object of the study is carbon steel of API 5L Grade A. The material was obtained from one of the oil and gas companies serving as the main oil lines. The working electrode was cut and cleansed using HCl 1M to obtain a smoother metal surface. The metal was then stored to remove the air contamination. It is presumed that the utilization of a soursop inhibitor is effective to modify the vulnerability of API 5L Grade A to corrosion in plentiful NaCl of produced water. Recent knowledge shows the phenolic derivates molecules bonding of –OH has greater adsorption than that of sole C-C and C-O bonds in carbon-based inhibitor molecules owing to the ease of formation of dative covalent bonds. This simplification can be adopted by controlling the reaction at cathodic and anodic regions through the evaluation of the optimum dose of inhibitor on the API 5L Grade A surface. Adding a combination between –OH, C=C, and C=O shares a common role to increase electron donations and extend the surface coverage protection inhibition area where corrodents have the least access.

4. 2. Preparation of soursop extraction solution and test solution

The extract of soursop was prepared by extraction process by cleaning the leaf before the surface area reached ±2 cm^2. Eventually, the leaf was dried at room temperature for seven days. The powdered leaf was obtained using a hammer mill and filtered with a 40–60 mesh. The powder was dried to maintain a water content of 15 % before it dissolved in ethanol and n-hexane. The ratio between the powder and the solution was 3:1, allowing it to stand for 24 hours. The solution was filtered to obtain the residue, which may redissolve using n-hexane and ethanol. The evaporation process continues to obtain the inhibitor extract using a rotary vacuum evaporator at 40 °C. The test solution comprises produced water of 10 ml where the concentration of the solution was prepared by adding 1, 2, 3, and 4 ml of the soursop extract.

4. 3. Potentiodynamic and Electrochemical Impedance Spectroscopy

The inhibitor measurement's polarization and Electrochemical Impedance Spectroscopy were selected to unveil the inhibitory performance. The working electrode was API 5L Grade A mounted to achieve a surface area of 1 cm^2 and earn a steady state for 1 hour. Pt and Ag/AgCl served as counter and reference electrodes (Metrohom, Switzerland). The polarization was measured between – 2 V to – 1.5 V compared to the reference electrode using the scanning rate of 20 mV/s. The result is depicted in the form of a Tafel Plot. The electrodes were immersed in the test solution according to ASTM G 95 [27] as shown in (1):

$$\left\{\eta=\frac{R_{inh}-R_s}{R_{inh}}\times 100\,\%\right\}. \quad (1)$$

Based on (1), R_{inh} and R_s correspond to inhibitor and solvent resistance.

In addition, the EIS applies the frequency between 100 kHz–10 mHz with the Open circuit potential (OCP) of 4 minutes. The obtained data were plotted using the Nyquist plot to analyze the interface mechanism between the substrate and test solution under ethanol and n-hexane solutions.

4. 4. Weight loss measurements

In this work, the weight loss measurement based on the ASTM G31-72 standard was carried out to unveil the corrosion process. The substrate was measured three times using an analytical balance with an accuracy of 0.2 mg. Upon immersing the metal under produced water, the weight loss was determined based on 3, 5, and 8 days. The observation was carried out in the absence and presence of inhibitors at 1, 2, and 4 ml. The mean value of the weight loss before and after the immersion test was repeated thrice to ensure measurement accuracy. Upon completion of the measurement, the sample was cleansed using HCl 5 % in an ultrasonic bath. The inhibition efficiency was calculated using (2) [28]:

$$\left\{\eta_w=\frac{v^0_{corr}-v_{corr}}{v^0_{corr}}\times 100\,\%\right\}, \quad (2)$$

where the corrosion rate was calculated using (3) [28]:

$$\left\{v_{corr}=\frac{\Delta W}{S\times t}\right\}. \quad (3)$$

According to (2) and (3), v^0_{corr} and v_{corr} are the corrosion rate without and with inhibitor (mmpy). ΔW is the weight difference, S is the exposure area, and t is the immersion time.

4. 5. Fourier-Transform Infrared Spectroscopy

In this study, the chemical structure of the soursop inhibitor was captured using FT-IR (Thermo Scientific Nicolet iS-10), Thermo Fisher Scientific, Waltham, MA. The working electrode was immersed in a test solution at 4 ml inhibitor for nearly 192 hours.

5. Results of using soursop as a green corrosion inhibitor

5. 1. Materials and their corrosion resistance results

5. 1. 1. Materials characterization

Table 1 shows the results of determining the chemical composition of the working electrode.

Table 1

Chemical composition of the working electrode

Fe (%)	C (%)	Si (%)	S (%)	P (%)	Cr (%)	Pb (%)
≈99.59	0.148	0.198	0.004	0.012	0.010	<0.025
Ni (%)	Mo (%)	Ti (%)	Cu (%)	Nb (%)	V (%)	Mn (%)
<0.005	0.008	<0.002	0.007	<0.002	<0.002	0.425

According to Table 1, the sample entails a carbon content of 0.148 % and is classified as low-carbon steel [29]. The

presence of Cr, Ni, Cu, Si, and Mo increases the corrosion resistance of the working electrode [30]. Despite their lower composition, it is vulnerable to corrosion.

5. 1. 2. Results of Potentiodynamic Polarization

Fig. 1 shows the results of polarization of the soursop inhibitor when extracted using ethanol and n-hexane.

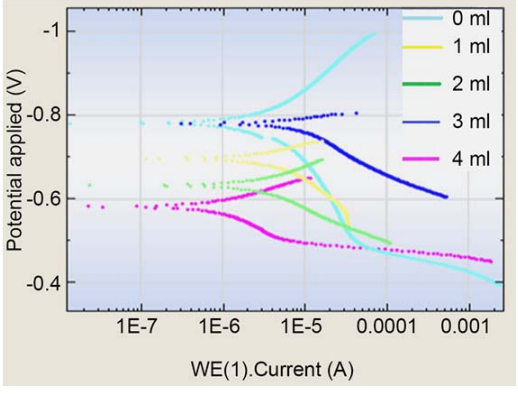

a

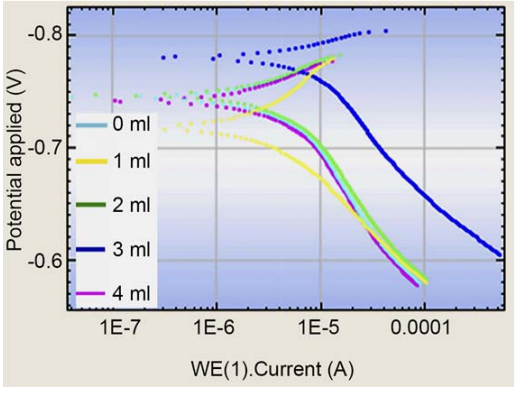

b

Fig. 1. Tafel Polarization of soursop dissolving in: *a* – ethanol; *b* – n-hexane

It is known that the polar solvent is critical to transfer all possible compounds into the solution, effectively influencing the inhibition process. It can be noted that the plot is essential to distinguish between the anodic and cathodic reactions before and after the addition of inhibitors. According to Fig. 1, *a*, the values of E_{corr} (potential corrosion) and i_{corr} (corrosion current density) decrease as a more concentrated inhibitor is added. Moreover, the current density reduction co-occurs at the anode and cathode when the API 5L Grade A substrate is added to the inhibitor in the ethanol solution.

Moreover, the Tafel plots of soursop dissolving in *n*-hexane shows minimum addition of inhibitor lowers the corrosion potential at 1 ml while the excessive solution is ineffective in reducing the effect of corrosion (Fig. 1, *b*). In the presence of various soursop concentrations, the corrosion current density shifted to a more negative region compared to the unprotecting substrate of about 0.1 μA at 4 ml of inhibitors. The inhibitor is classified as a mixed-type inhibitor affecting both solvents' cathodic and anodic areas.

Tables 2, 3 agree well with Fig. 1, which explains the nature of soursop inhibition.

Table 2

Results of soursop inhibitor under ethanol solvent

Solution	Inhibitor concentration (mL)	Ecorr (mv vs Ag/AgCl)	Corr Rate (mm/yr)	% E. I.
Produced water	0	–788.95	0.1321	–
	1	–697.66	0.0682	48.15
	2	–643.69	0.0433	67.09
	3	–806.42	0.1030	21.85
	4	–586.53	0.0155	88.25

It can be noted that at a higher concentration of 4 ml, the inhibitor is practical to put the extra barrier between the bare metal and produced water (88.25 %). The remarkable efficiency agrees well with the depression of corrosion rate at 0.0155 mmpy and more negative E_{corr} at –586.53 mV compared to Ag/AgCl (Table 2). Moreover, Table 2 shows that the value of E_{corr} at 3 ml of inhibitor gives the potential at –806.42 mV, which was higher than the remaining volume of inhibitor. In this case, the value of corrosion potential favors the cathodic region despite the remaining solution proceeding to the anodic site. Table 3 shows the effect of the inhibitor when extracted using n-hexane.

Table 3

Results of soursop inhibitor under n-hexane solvent

Solution	Inhibitor concentration (mL)	Ecorr (mv vs Ag/AgCl)	Corr Rate (mm/yr)	% E.I.
Produced water	0	–788.95	0.13165	–
	1	–727.09	0.05460	58.52
	2	–762.27	0.07910	39.90
	3	–761.79	0.07643	41.93
	4	–758.93	0.07732	41.26

Table 3 illustrates that the value of E_{corr} is generally similar with different corrosion rates while the increasing concentration of inhibitor fails to elevate their inhibition efficiency. Despite the depression of inhibition efficiency (41.2 %), the inhibitor relatively depresses the electrochemical process with approximately 50 % smaller corrosion rate (Table 3) compared to those without an inhibitor. In essence, the difference in corrosion potential between the uninhibited and inhibited solution for ethanol solvent was greater than ± 85 mV and associated with the mixed-type inhibitor. It can be concluded that this behavior is inherent in the inhibitor when immersed in ethanol only while the same solution showcases a different property under n-hexane solution. It may be correlated to the lower inhibition efficiency of 58.52 % and continuously decreases upon the addition of the larger volume of inhibitor.

5. 1. 3. Results of Electrochemical Impedance Spectroscopy

The anti-corrosion performance of the soursop inhibitor, when the substrate is immersed in the test solution, was performed to research the electrochemical process on the surface of API 5L Grade A. Fig. 2 shows the test results related to corrosion protection of the natural inhibitor.

According to Fig. 2, the Nyquist curves show the presence of the incomplete half-loop with a one-time constant. The loop diameter of the Nyquist plot without inhibitor is larger than that of the 3 ml solution, while the shape of all plots remains similar. Moreover, the depression of the semi-

circular arc shape also increases as the inhibitor concentration shows the mechanistic inhibition is identical. In this case, the 3 ml solution of inhibitor orients in a vertical orientation and creates instability of the inhibitor to attach to the substrate

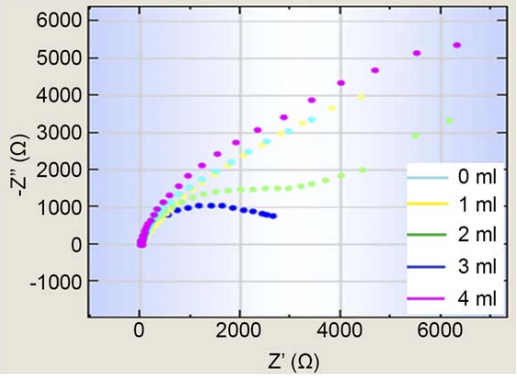

Fig. 2. Results of the soursop inhibitor Electrochemical Impedance Spectroscopy

surface [29].

In addition, Table 4 showcases the results of the solution resistance (R_s), charge transfer resistance (R_{ct}), and double-layer capacitance (C_{dl}).

Table 4

Results of Electrochemical Impedance Spectroscopy

Conc (mL)	R_{ct} (Ω·cm^{-2})	R_s (Ω·cm^{-2})	C_{dl} (μF·cm^{-2})
0	38.3	39.8	552
1	18.1	3.03	599
2	24.9	1.19	360
3	19.1	29.7	377
4	16.1	2.69	31

The value of double-layer capacitance decreases as the concentration increases (552 to 31 μF·cm^{-2}) to demonstrate the adsorption of the inhibitor [30]. With this in mind, it can be noted that more inhibitors solidified to form a thick inhibitor layer as more soursop is added.

5. 1. 4. Results of weight loss measurement

Tables 5–7 compare the results of gravimetric weight loss measurement carried out on the API 5L Grade A coupons with rectangular shape under produced water (unprotected and protected) with 72, 120, and 192 days immersion time.

Table 5

Results of immersion test for 72 hours

Conc (mL)	Time (hour)	Initial weight (g)	Final weight (g)	Weight loss (mg)	Corr rate (mpy)	Average Corr rate (mpy)	EI (%)
A 0	72	12.164	12.142	0.0217	10.735	9.788	–
B 0	72	12.828	12.811	0.0172	8.841		–
C 1	72	11.988	11.967	0.0207	10.641	10.120	0.88
D 1	72	11.927	11.909	0.0178	9.600		10.5
E 2	72	12.050	12.037	0.0127	6.283	8.4845	41.474
F 2	72	13.068	13.046	0.0216	10.686		0.460
G 4	72	12.360	12.342	0.0181	8.954	8.311	16.589
H 4	72	11.653	11.637	0.0155	7.668		28.571

Table 6

Results of immersion test for 120 hours

Conc (mL)	Time (hour)	Initial weight (g)	Final weight (g)	Weight loss (mg)	Corr rate (mpy)	Average Corr rate (mpy)	EI (%)
I 0	120	13.251	13.245	0.0064	1.84	1.865	–
J 0	120	13.239	13.232	0.0066	1.89		–
K 1	120	13.388	13.384	0.0036	1.03	1.04	45.454
L 1	120	13.025	13.022	0.0037	1.05		44.485
M 2	120	13.038	13.034	0.0039	1.12	1.12	40.909
N 2	120	11.573	11.569	0.0039	1.12		40.909
O 4	120	11.335	11.331	0.0046	1.32	1.27	30.303
P 4	120	11.730	11.725	0.0043	1.23		34.848

Table 7

Results of immersion test for 192 hours

Conc (mL)	Time (hour)	Initial weight (g)	Final weight (g)	Weight loss (mg)	Corr rate (mpy)	Average Corr rate (mpy)	EI (%)
Q 0	192	12.2685	12.260	0.0078	1.422	1.577	–
R 0	192	12.2460	12.236	0.0095	1.732		–
S 1	192	13.348	13.342	0.0057	1.039	0.966	40.00
T 1	192	12.473	12.468	0.0049	0.893		48.42
U 2	192	13.068	12.029	0.0048	0.875	0.8475	49.47
V 2	192	12.033	12.208	0.0045	0.820		52.63
W 4	192	11.653	12.201	0.0049	0.893	0.948	48.42
Y 4	192	12.206	11.614	0.0055	1.003		42.10

In this work, the coupon was duplicated to compare the inhibition efficiency and corrosion rate under the same conditions. The code of A-Y was attached to the inhibitor concentration. Overall, the corrosion rate of the protected substrate decreases as the concentration increases while the inhibition efficiency increases as a function of time. The highest inhibition efficiency was achieved with a 2 ml solution when the metal was immersed for 192 hours at 52.63 % (Table 7). In comparison, the test solution of 4 ml inhibitor after 72 hours of inhibition shows the lowest performance at 0.460 % (Table 5). Despite the above results, adding the soursop inhibitor of 1, 2, and 4 ml in the produced water with the inhibitor shows a lower yellow color intensity than without inhibitor solution protection.

5. 2. Results of functional group identification

Fig. 3 depicts the spectrum information related to the FTIR spectra of the soursop inhibitor.

The effect of soursop in pure extract shows the absorption of several functional groups. The hydroxyl (–O.H.) absorption appears at 3.361 cm^{-1} while the stretching of C=O aromatic appearance is obvious at relatively strong absorption at 2.919 cm^{-1} and is confirmed similar to [31] (Fig. 3, *a*). The bond C=C stretch asymmetric is accountable for the peak absorption of 1.604 cm^{-1}. The peak at 1,441 corresponds to –O.H. bending due to alcohol and phenolic compounds [32].

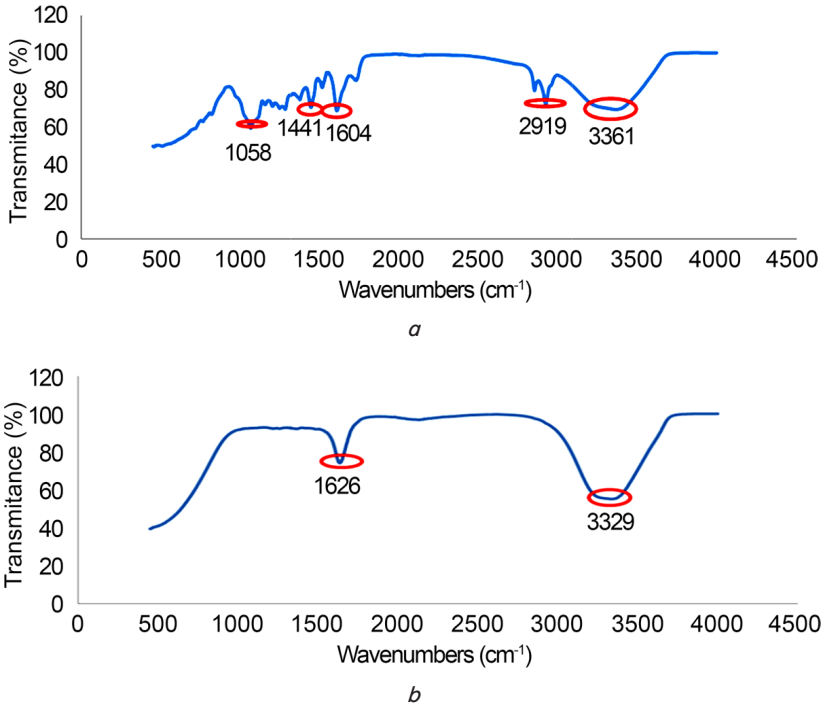

Fig. 3. Results of functional group identification spectrum: *a* – pure inhibitor extract; *b* – API 5L grade A immersed in inhibitor

Moreover, the wavenumber of 1,058 cm^{-1} suggests the rise of ether stretching.

On the contrary, the absorption of several functional groups significantly impacts the inhibition mechanism of the inhibitor. The remaining appearance peak at 3.329 cm^{-1} and 1.626 cm^{-1} suggests an excessive amount of –O.H. and C=C. It is predicted to be inherent in the molecules of soursop.

At the same time, the disappearance of the rest functional groups suspected has wholly attached to the surface of API 5L Grade A and forms a new passive layer of protection against corrodents.

5. 3. Adsorption Isotherm Studies

The mechanism of inhibitor attachment on the substrate can be studied using the adsorption isotherm model to unveil the surface interaction. In this work, the Langmuir, Temkin, and Frumkin models show variation in isotherm adsorption to determine the extension of inhibitor corrosion on the surface of the substrate. In this case, the suitability of the fitting model is assessed to determine the equilibrium adsorption constant, K_{ads} using (4)–(6) [33]:

$$\left\{\frac{c}{\theta}=\frac{1}{K_{ads}}+C\right\}, \quad (4)$$

$$\{\theta=\ln C_R+K_{ads}\}, \quad (5)$$

$$\left\{\log\left\{\frac{\theta}{1-\theta}\right\}C_R=2.303\log K_{ads}+g\theta\right\}. \quad (6)$$

In the above Equation, θ, C_R, $K_{ads,}$ and g are the surface coverage, inhibitor concentration (mol·dm^{-3}), and adsorbate parameter. Table 5 compares the adsorption isotherm parameters based on the above equation.

It is possible to vary the plotting C/θ (y-axis) vs θ (x-axis), log C/θ vs θ, and log $\theta/(1-\theta)C$ vs θ to provide the model of each adsorption isotherm model. The obtained value of R^2 concerning identifying the most typical isotherm adsorption model is given based on Table 5. Doubling the inhibitor's volume increases the surface coverage area of protection from 0.401 to 0.495, indicating that the inhibitor adsorbed on the surface of metals (Table 5). Nevertheless, the inhibition gradually decreased at 4 ml of inhibitor, causing lower protection on the bare metal. According to the above calculation, various adsorption isotherm plot is produced and presented in Fig. 4–6 after 8 days of immersion.

According to Fig. 4 and (4)–(6), the obtained value of R^2 is 0.9713, 0.0053, and 0.0525 for the Langmuir, Temkin, and Frumkin adsorption isotherm models. The nearness of R^2 to 1 shows that the soursop inhibitor most likely adheres to the Langmuir isotherm model.

Table 5

Adsorption isotherm calculation

C (ml)	*Corr rate* (mmpy)	*E.I.* (%)	θ	C/θ	Log C/θ	log $\theta/(1-\theta)$ C
1	1.039	40.1	0.401	2.5	–0.397	–0.176
1	0.893	48.42	0.484	2.083	–0.315	–0.028
2	0.875	49.47	0.495	4.048	–0.606	–0.311
2	0.82	52.63	0.526	3.8	–0.581	–0.255
4	0.893	48.42	0.484	8.264	–0.917	–0.593
4	1.003	42.11	0.421	9.501	–0.977	–0.741

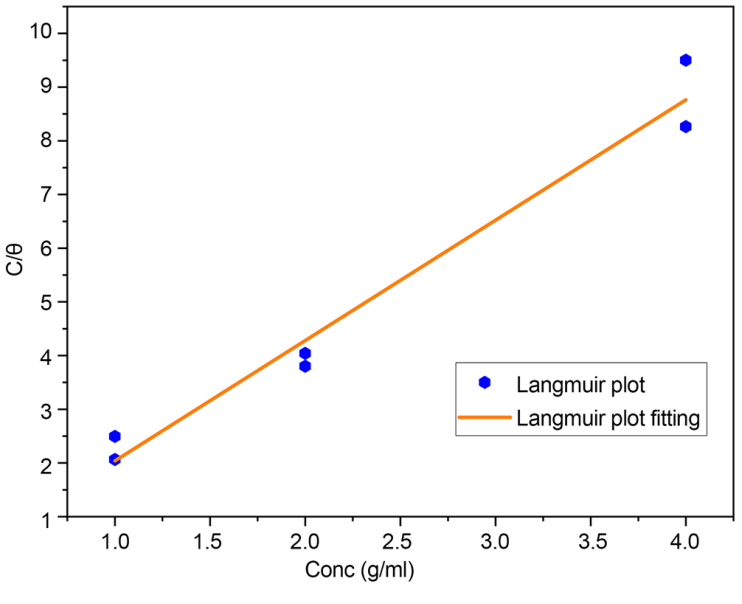

Fig. 4. Langmuir adsorption isotherm model plot

6. Discussion of the results of the study of *Annona muricata Linn* as a green corrosion inhibitor

The anticorrosion inhibition of the soursop solution and the electrochemical inhibition processes of the API 5L Grade B steel electrode in produced water in the presence and absence of inhibitors at various concentrations were studied by potentiodynamic and EIS. Of varied concentrations, the optimum inhibition was achieved by adding ethanol at 4 ml to show that ethanol has polar and polar interaction to provide maximum extraction. The corrosion potential shifting from a negative to a positive region of –788.95 mV to –586.53 mV offers the feature of an anodic inhibitor. In contrast, the addition of 3 ml of inhibitor shows a mixed-type inhibitor, which interrupts the evolution of hydrogen gas and dissolution of bare metal under produced water [34]. High extraction mode shows that ethanol best extracts all the functional groups exhibited in the soursop inhibitor. Notably, the compounds are prominent and preferentially leached out since they are suspected of interacting due to polar-polar bonding [35]. At the same time, a small amount of inhibitor could not inhibit the oxidation process due to a lower change in corrosion rate despite the higher volume injected in the test solution. Adsorption is the key to inhibition, lowering the corrosion current density to a negative value. In addition, the corrosion inhibitor in ethanol solution shows the irregular Tafel plot change due to the soursop adsorption on the active site of the bare metals.

The results of Nyquist plots show that the capacitance of the arc has similar shapes except for the 2 ml solution (Fig. 2). As such, it can be concluded that the inhibitor exhibits the likeliness to inhibit the reaction at the cathode and anode by a similar mechanism [36]. Particularly, the inhibitor has been adsorbing on the metal while the diameter of capacitance increases remarkably with the increase of soursop concentration. The increase in diameter implies that the inhibitor has a greater inhibition capacity despite the oblate shape at 4 ml inhibitor. In this case, the presence of inhibitor shows a frequency dispersion corresponding to the heterogeneous and rougher surface [37]. The Nyquist plot's result aligns with the EIS result, which shows that the value of C_{dl} decreases (Table 4). Based on Table 4, the rise in charge transfer resistance, R_{ct}, and the concurrent decrease of C_{dl} correlate with the displacement of more water molecules in the produced water and an increase in the protection of the metal from corrodents.

Moreover, the weight loss result shows the reduction of corrosion in various media at different immersion times. According to Tables 5–7, the immersion of three days shows the highest efficiency with the optimum of 2 ml of inhibitor. The result opposes polarization, which may have a linear rise as concentration increases. It is suspected that the produced water is contaminated with H_2S. The weak acid darkens the coupon and inhibits the adsorption of the inhibitor on the surface of API 5L Grade A. A shorter immersion time is also predicted to give better protection since the remaining compound is fully adsorbed at the active sites [38].

On the contrary, the result of five days of immersion time shows a rise in concentration provides the optimum corrosion rate. In addition, the inhibition efficiency remains lower at 52.63 % at 2 ml of inhibitor after eight days of immersion. This implies that the inhibitor molecule's adsorption was partially attached to the surface of the coupon.

In this case, the lack of protection may correlate to the shortage of functional groups such as C=O, –O.H., C–O–C, and delocalization of C=C (Fig. 3). The intense peak of the above compound increases the hydrogen bonding between the extract of soursop and produced water. Notably, the primary representation of the phenolic compound in soursop provides an electron-donating process from the inhibitor to the metal, which indicates the adsorption process [39]. The C=C double bond contributes to the inhibitor's likelihood to provide a pair of electrons to form a dative covalent bond.

The adsorption of an inhibitor can be modeled using Frumkin, Langmuir, and Temkin models. According to Fig. 4, the R^2 value of 0.9731 implies the soursop molecule could be fitted to the Langmuir isotherm adsorption model. In this model, it is presumed that the inhibition occurs at the interface between the substrate and solution involving chemical and physical bonding [40]. Comparing another fitting plot of linear regression shows that R^2 is more negligible by 0.0053 and 0.0525, and the slope is 0.4108 and 1.2873 for Temkin and Frumkin. Hence, the Langmuir model shows that the exposed surface area has been completed and attached with numerous compounds, which appeared in Fig. 3 [41].

It is noteworthy to discuss the potential effect of using soursop as a green corrosion inhibitor. It is believed that the protective effect of soursop film inhibitor is effective against produced water-induced corrosion through chemical and physical mechanisms. From the perspective of the corrosion test, the addition of a soursop inhibitor effectively reduces the cathodic and anodic reactions. Therefore, the surface of API 5L Grade A is denser than that of bare metal. The extensive protective dense layer slows down the adhesion of chloride and their corresponding corrodent on the surface of the substrate, thus achieving the physical effect of anti-corrosion. In this circumstance, it is possible to direct the forthcoming research to unveil the effect of the sole chemical content of soursop and how to delve into their mechanism. While using molecular dynamic simulation is critical, the implementation of machine learning offers an extensive contribution by utilizing numerical data from polarization tests.

Despite the results of the characterization and inhibition, it is noteworthy to note the limitation of the work is the lack of study of surface morphology. This drawback is inherent in the uncertain coating process of the abundance of active sites. It is also essential to include the calculation of the surface roughness of the inhibition to understand the model entirely. Nevertheless, the successive study should also assess the effect of temperature on the adsorption model.

7. Conclusions

1. The primary functional group of inhibitors shows the presence of C=O (2.919 cm^{-1}), C=C (1.604 cm^{-1}), -OH (3.361 cm^{-1}), and phenolic compounds (1441 cm^{-1}), which indicates the strengthening of the bonding qualitatively. Hence, the adsorption is enhanced and available for protecting the metal from the corrodent due to chemical bonding.

2. Ethanol and n-hexane are critical substances to extracting the soursop's active content. The corrosion test reveals the moderately high inhibition efficiency at 88.25 % correlated to the charge transfer process and a decrease in the double-layer capacitance at 31 $\mu F.cm^{-2}$ in most inhibitor concentrations. At the same time, the charge transfer resistance increases except for the 2 ml inhibitor. The optimum

condition of the inhibitor to restore the protection of metals based on weight loss is three days with a lower corrosion rate at 7.668 mpy with an indication of quantitative indicator towards the result of the research.

3. The adsorption of inhibitor employs the Langmuir model that shows the formation of the heterogeneous passive layer to cover the substrate due to the nearness of the R^2 value to 1. This study indicates that the inhibitor effectively recovers pit corrosion due to the qualitatively dissolving metal.

Conflict of interest

The authors declare that they have no conflict of interest with this research, whether financial, personal, authorship or otherwise, that could affect the study and its results presented in this paper.

Financing

The authors thank the Akamigas Energy and Mineral Polytechnic with contract number 027/SP3/Penelitian/DIPA2023/PEM Akamigas.

Data availability

Data cannot be made available for reasons disclosed in the data availability Statement.

Acknowledgments

The authors are grateful to the Indonesian Akamigas Energy and Mineral Polytechnic, CEPU of Indonesia.

References

1. Liu, H., Gu, T., Zhang, G., Wang, W., Dong, S., Cheng, Y., Liu, H. (2016). Corrosion inhibition of carbon steel in CO2-containing oilfield produced water in the presence of iron-oxidizing bacteria and inhibitors. Corrosion Science, 105, 149–160. doi: https://doi.org/10.1016/j.corsci.2016.01.012
2. Verma, C., Ebenso, E. E., Bahadur, I., Quraishi, M. A. (2018). An overview on plant extracts as environmental sustainable and green corrosion inhibitors for metals and alloys in aggressive corrosive media. Journal of Molecular Liquids, 266, 577–590. doi: https://doi.org/10.1016/j.molliq.2018.06.110
3. Fakhru'l-Razi, A., Pendashteh, A., Abdullah, L. C., Biak, D. R. A., Madaeni, S. S., Abidin, Z. Z. (2009). Review of technologies for oil and gas produced water treatment. Journal of Hazardous Materials, 170 (2-3), 530–551. doi: https://doi.org/10.1016/j.jhazmat.2009.05.044
4. Ottaviano, J. G., Cai, J., Murphy, R. S. (2014). Assessing the decontamination efficiency of a three-component flocculating system in the treatment of oilfield-produced water. Water Research, 52, 122–130. doi: https://doi.org/10.1016/j.watres.2014.01.004
5. Nesrine, L., Salima, K., Lamine, K. M., Belaid, L., Souad, Bk., Lamine, G. M. et al. (2020). Phylogenetic characterization and screening of halophilic bacteria from Algerian salt lake for the production of biosurfactant and enzymes. World Journal of Biology and Biotechnology, 5 (2), 1. doi: https://doi.org/10.33865/wjb.005.02.0294
6. Neff, J., Lee, K., DeBlois, E. M. (2011). Produced Water: Overview of Composition, Fates, and Effects. Produced Water, 3–54. doi: https://doi.org/10.1007/978-1-4614-0046-2_1
7. Jiménez, S., Micó, M. M., Arnaldos, M., Medina, F., Contreras, S. (2018). State of the art of produced water treatment. Chemosphere, 192, 186–208. doi: https://doi.org/10.1016/j.chemosphere.2017.10.139
8. Azmi, M. F., Soedarsono, J. W. (2018). Study of corrosion resistrance of pipeline API 5L X42 using green inhibitor bawang dayak (Eleutherine americanna Merr.) in 1M HCl. IOP Conference Series: Earth and Environmental Science, 105, 012061. doi: https://doi.org/10.1088/1755-1315/105/1/012061
9. Arlan, A. S., Subekti, N., Soedarsono, J. W., Rustandi, A. (2018). Corrosion Inhibition by a Caesalpinia Sappan L Modified Imidazoline for Carbon Steel API 5L Grade X60 in HCl 1M Environment. Materials Science Forum, 929, 158–170. doi: https://doi.org/10.4028/www.scientific.net/msf.929.158
10. Kaban, A. P. S., Ridhova, A., Priyotomo, G., Elya, B., Maksum, A., Sadeli, Y. et al. (2021). Development of white tea extract as green corrosion inhibitor in mild steel under 1 M hydrochloric acid solution. Eastern-European Journal of Enterprise Technologies, 2 (6 (110)), 6–20. doi: https://doi.org/10.15587/1729-4061.2021.224435
11. Kaban, A., Mayangsari, W., Anwar, M., Maksum, A., Aditiyawarman, T., Soedarsono, J. et al. (2022). Unraveling the study of liquid smoke from rice husks as a green corrosion inhibitor in mild steel under 1 M HCl. Eastern-European Journal of Enterprise Technologies, 5 (6 (119)), 41–53. doi: https://doi.org/10.15587/1729-4061.2022.265086
12. Gurjar, S., Sharma, S. K., Sharma, A., Ratnani, S. (2021). Performance of imidazolium based ionic liquids as corrosion inhibitors in acidic medium: A review. Applied Surface Science Advances, 6, 100170. doi: https://doi.org/10.1016/j.apsadv.2021.100170
13. Mo, S., Li, L. J., Luo, H. Q., Li, N. B. (2017). An example of green copper corrosion inhibitors derived from flavor and medicine: Vanillin and isoniazid. Journal of Molecular Liquids, 242, 822–830. doi: https://doi.org/10.1016/j.molliq.2017.07.081
14. Lu, H., Huang, K., Azimi, M., Guo, L. (2019). Blockchain Technology in the Oil and Gas Industry: A Review of Applications, Opportunities, Challenges, and Risks. IEEE Access, 7, 41426–41444. doi: https://doi.org/10.1109/access.2019.2907695
15. Hasmila, I., Natsir, H., Soekamto, N. H. (2019). Phytochemical analysis and antioxidant activity of soursop leaf extract (Annona muricata Linn.). Journal of Physics: Conference Series, 1341 (3), 032027. doi: https://doi.org/10.1088/1742-6596/1341/3/032027

16. Uwah, I. E., Okafor, P. C., Ebiekpe, V. E. (2013). Inhibitive action of ethanol extracts from Nauclea latifolia on the corrosion of mild steel in H2SO4 solutions and their adsorption characteristics. Arabian Journal of Chemistry, 6 (3), 285–293. doi: https://doi.org/10.1016/j.arabjc.2010.10.008
17. Valdez-Salas, B., Vazquez-Delgado, R., Salvador-Carlos, J., Beltran-Partida, E., Salinas-Martinez, R., Cheng, N., Curiel-Alvarez, M. (2021). Azadirachta indica Leaf Extract as Green Corrosion Inhibitor for Reinforced Concrete Structures: Corrosion Effectiveness against Commercial Corrosion Inhibitors and Concrete Integrity. Materials, 14 (12), 3326. doi: https://doi.org/10.3390/ma14123326
18. Saratha, R., Vasudha, V. G. (2010). Emblica Officinalis (Indian Gooseberry) Leaves Extract as Corrosion Inhibitor for Mild Steel in 1N HCl Medium. E-Journal of Chemistry, 7 (3), 677–684. doi: https://doi.org/10.1155/2010/162375
19. Okafor, P. C., Uwah, I. E., Ekerenam, O. O., Ekpe, U. J. (2009). Combretum bracteosum extracts as eco-friendly corrosion inhibitor for mild steel in acidic medium. Pigment & Resin Technology, 38 (4), 236–241. doi: https://doi.org/10.1108/03699420910973323
20. Haldhar, R., Prasad, D., Bhardwaj, N. (2019). Extraction and experimental studies of Citrus aurantifolia as an economical and green corrosion inhibitor for mild steel in acidic media. Journal of Adhesion Science and Technology, 33 (11), 1169–1183. doi: https://doi.org/10.1080/01694243.2019.1585030
21. Abdellattif, M. H., Alrefaee, S. H., Dagdag, O., Verma, C., Quraishi, M. A. (2021). Calotropis procera extract as an environmental friendly corrosion Inhibitor: Computational demonstrations. Journal of Molecular Liquids, 337, 116954. doi: https://doi.org/10.1016/j.molliq.2021.116954
22. Widyastuti, D. A., Rahayu, P. (2017). Antioxidant Capacity Comparison of Ethanolic Extract of Soursop (Annona muricata Linn.) Leaves and Seeds as Cancer Prevention Candidate. Biology, Medicine, & Natural Product Chemistry, 6 (1), 1. doi: https://doi.org/10.14421/biomedich.2017.61.1-4
23. Riastuti, R., Setiawidiani, D., Soedarsono, J. W., Aribowo, S., Kaban, A. P. S. (2022). Development of saga (Abrus precatorius) seed extract as a green corrosion inhibitor in API 5l Grade B under 1m HCL solutions. Eastern-European Journal of Enterprise Technologies, 4 (6 (118)), 46–56. doi: https://doi.org/10.15587/1729-4061.2022.263236
24. Kaban, E. E., Maksum, A., Permana, S., Soedarsono, J. W. (2018). Utilization of secang heartwood (caesalpinia sappan l) as a green corrosion inhibitor on carbon steel (API 5L Gr. B) in 3.5% NaCl environment. IOP Conference Series: Earth and Environmental Science, 105, 012062. doi: https://doi.org/10.1088/1755-1315/105/1/012062
25. Ayende, Rustandi, A., Soedarsono, J. W., Priadi, D., Sulistijono, Suprapta, D. N., Priyotomo, G., Bakri, R. (2014). Interaction of Purple Sweet Potato Extract with Ascorbic Acid in FeCl3 Solution. Applied Mechanics and Materials, 680, 32–37. doi: https://doi.org/10.4028/www.scientific.net/amm.680.32
26. Xie, M. (2021). Castor-Bean Extract as an Inhibitor for Low Carbon Steel Corrosion in Simulated Oilfield Produced Water. International Journal of Electrochemical Science. doi: https://doi.org/10.20964/2021.08.24
27. Standard Reference Test Method for Making Potentiostatic and Potentiodynamic Anodic Polarization Measurements (1994). ASTM.
28. Zheng, Z., Hu, J., Eliaz, N., Zhou, L., Yuan, X., Zhong, X. (2022). Mercaptopropionic acid-modified oleic imidazoline as a highly efficient corrosion inhibitor for carbon steel in CO2-saturated formation water. Corrosion Science, 194, 109930. doi: https://doi.org/10.1016/j.corsci.2021.109930
29. Chauhan, D. S., Quraishi, M. A., Srivastava, V., Haque, J., Ibrahimi, B. E. (2021). Virgin and chemically functionalized amino acids as green corrosion inhibitors: Influence of molecular structure through experimental and in silico studies. Journal of Molecular Structure, 1226, 129259. doi: https://doi.org/10.1016/j.molstruc.2020.129259
30. Attou, A., Tourabi, M., Benikdes, A., Benali, O., Ouici, H. B., Benhiba, F. et al. (2020). Experimental studies and computational exploration on the 2-amino-5-(2-methoxyphenyl)-1,3,4-thiadiazole as novel corrosion inhibitor for mild steel in acidic environment. Colloids and Surfaces A: Physicochemical and Engineering Aspects, 604, 125320. doi: https://doi.org/10.1016/j.colsurfa.2020.125320
31. Chen, Z., Wang, M., Fadhil, A. A., Fu, C., Chen, T., Chen, M. et al. (2021). Preparation, characterization, and corrosion inhibition performance of graphene oxide quantum dots for Q235 steel in 1 M hydrochloric acid solution. Colloids and Surfaces A: Physicochemical and Engineering Aspects, 627, 127209. doi: https://doi.org/10.1016/j.colsurfa.2021.127209
32. Galai, M., Rbaa, M., Ouakki, M., Abousalem, A. S., Ech-chihbi, E., Dahmani, K. et al. (2020). Chemically functionalized of 8-hydroxyquinoline derivatives as efficient corrosion inhibition for steel in 1.0 M HCl solution: Experimental and theoretical studies. Surfaces and Interfaces, 21, 100695. doi: https://doi.org/10.1016/j.surfin.2020.100695
33. Rekkab, S. et al. (2012). Green corrosion inhibitor from essential oil of eucalyptus globulus (Myrtaceae) for C38 steel in sulfuric acid solution. J. Mater. Environ. Sci., 3 (4), 613–627. Available at: https://www.jmaterenvironsci.com/Document/vol3/vol3_N4/61-JMES-269-2012-Rekkab.pdf
34. Paul Setiawan Kaban, A., Mayangsari, W., Syaiful Anwar, M., Maksum, A., Riastuti, R., Aditiyawarman, T., Wahyuadi Soedarsono, J. (2022). Experimental and modelling waste rice husk ash as a novel green corrosion inhibitor under acidic environment. Materials Today: Proceedings, 62, 4225–4234. doi: https://doi.org/10.1016/j.matpr.2022.04.738
35. Melo, T., Figueiredo, A. R. P., da Costa, E., Couto, D., Silva, J., Domingues, M. R., Domingues, P. (2021). Ethanol Extraction of Polar Lipids from Nannochloropsis oceanica for Food, Feed, and Biotechnology Applications Evaluated Using Lipidomic Approaches. Marine Drugs, 19 (11), 593. doi: https://doi.org/10.3390/md19110593

36. Tourabi, M., Nohair, K., Traisnel, M., Jama, C., Bentiss, F. (2013). Electrochemical and XPS studies of the corrosion inhibition of carbon steel in hydrochloric acid pickling solutions by 3,5-bis(2-thienylmethyl)-4-amino-1,2,4-triazole. Corrosion Science, 75, 123–133. doi: https://doi.org/10.1016/j.corsci.2013.05.023
37. Baux, J., Caussé, N., Esvan, J., Delaunay, S., Tireau, J., Roy, M. et al. (2018). Impedance analysis of film-forming amines for the corrosion protection of a carbon steel. Electrochimica Acta, 283, 699–707. doi: https://doi.org/10.1016/j.electacta.2018.06.189
38. Chowdhury, M. A., Ahmed, M. M. S., Hossain, N., Islam, M. A., Islam, S., Rana, M. M. (2023). Tulsi and green tea extracts as efficient green corrosion inhibitor for the corrosion of aluminum alloy in acidic medium. Results in Engineering, 17, 100996. doi: https://doi.org/10.1016/j.rineng.2023.100996
39. Vasyliev, G. S., Vorobyova, V. I., Linyucheva, O. V. (2020). Evaluation of Reducing Ability and Antioxidant Activity of Fruit Pomace Extracts by Spectrophotometric and Electrochemical Methods. Journal of Analytical Methods in Chemistry, 2020, 1–16. doi: https://doi.org/10.1155/2020/8869436
40. Bhardwaj, N., Sharma, P., Kumar, V. (2021). Phytochemicals as steel corrosion inhibitor: an insight into mechanism. Corrosion Reviews, 39 (1), 27–41. doi: https://doi.org/10.1515/corrrev-2020-0046
41. Yaro, A. S., Khadom, A. A., Wael, R. K. (2013). Apricot juice as green corrosion inhibitor of mild steel in phosphoric acid. Alexandria Engineering Journal, 52 (1), 129–135. doi: https://doi.org/10.1016/j.aej.2012.11.001